Experimental and Theoretical Investigation of HC_5N Adsorption on Amorphous Ice Surface: Simulation of the Interstellar Chemistry

Anne Coupeaud, Nathalie Piétri, Alain Allouche, Jean-Pierre Aycard, and Isabelle Couturier-Tamburelli*

UMR CNRS 6633, Physique des Interactions Ioniques et Moléculaires, Equipe de Spectrométries et Dynamique Moléculaires, Université de Provence, Case 252, Centre de St-Jérôme, 13397 Marseille cedex 20, France

Received: April 23, 2008; Revised Manuscript Received: July 1, 2008

HC_5N adsorbed on amorphous water ice at 10 K presents an interaction with the ice surface and induces the restructuring of the ice amorphous bulk. Warming up the sample induces the HC_5N desorption from the H_2O ice film, between 120 and 160 K, and the associated desorption energy is 90 kJ/mol. This value is in good agreement with that calculated E_d (80 kJ/mol) and gives evidence that the amorphous ice surface is essentially dynamic. From theoretical calculations, it is shown that the HC_5N moiety presents a curvature and is no more linear and stabilized by two strong N···H bonds (2.09 and 2.29 Å) and one H···O bond (1.84 Å).

Introduction

At the present time, around 130 molecular species, neglecting isotopic variants, have been detected in interstellar clouds and circumstellar regions. Most molecules are detected in the opaque circumstellar envelopes of stars, among these molecules long carbon-chain molecules and cyanopolyynes (HC_nN with $n = 3-11$) have also been observed in these areas.[1]

The rich chemistry of this medium results in the variety of physical conditions of the various interstellar objects. The emission of stellar UV photons drives a quickly evolving photochemistry. To understand the active chemistry that takes place on grain mantles (constituted by a silicate and/or carbonaceous core surrounded by an ice mantle, the latter essentially constituted of water), numerous laboratory models have been developed.

Furthermore, Titan, the largest Saturnian satellite, has a dense atmosphere similar to the terrestrial one, essentially composed of N_2 ($\geq$90%) and CH_4 ($\approx$2%), which allows nitrile formation under UV photon irradiations.[2] Up to this day, four gas-phase nitriles have already been identified in Titan's atmosphere: HCN, CH_3CN, HC_3N, and C_2N_2. The fifth one, C_4N_2, has been detected as a solid.[3] These compounds are essential for the synthesis of amino acids and are particularly helpful for understanding Titan's chemistry and probably also that of the early Earth. Since the detection of H_2O in the Titan's atmosphere,[4] we can suppose that water ice can play a role in the chemistry of species adsorbed or trapped in its lattice. Ever since its discovery in space,[5] the cyanodiacetylene (2,4-pentadiynenitrile and 1-cyano-1,3-butadiyne) has drawn the attention of spectroscopists and astrochemists. It is also a potential constituent of the atmosphere of Titan and has been found in laboratory simulations with Titan-like gas mixtures.[6]

In previous papers,[7,8] the results of the structure and energy of 1:1 complexes formed between cyanopolyynes (HC_5N and HC_3N) and water in argon matrix have been presented. Two kinds of complexes were observed, with water playing the role of either acceptor or donor of a proton.

The purpose of the present work is to assess the chemical stability of HC_5N adsorbed on water ice surface and to describe the nature of the adsorption sites of HC_5N on amorphous water ice. We wanted to answer the question "does HC_5N interact with water ice like HC_3N or C_4N_2?"

Experimental Section

Pure cyanobutadiyne was synthesized using the method described by Trolez and Guillemin.[9] The sample was distilled before each deposition. Moreover, the first fraction of HC_5N was always eliminated. H_2O was doubly distilled before use.

Low-density amorphous ice films were obtained from a water/argon (1/50) gaseous mixture deposited on a highly polished Au-platted copper cube held at 80 K. The deposition was made under pumping to 10^{-7} mbar to outgas Ar and obtain a porous solid.[10] Then, the ice film was recooled to 10 K to deposit pure HC_5N (ca. 5 μmol, corresponding approximatively to a monolayer) and to study the adsorption process. Adsorption and desorption of HC_5N on the amorphous ice film were monitored by infrared spectroscopy using a Nicolet series II Magma system 750 in the 4000 to 650 cm^{-1} wavenumber range at a resolution of 1 cm^{-1}.

Infrared spectra of amorphous ice have been extensively described in the literature.[11] Above 80 K, during a temperature increase, an irreversible modification of the amorphous ice toward crystalline form was observed near 145 K. Ice remains crystalline, until the sample sublimation at 180 K. This form is characterized by shoulders[12] at 3340 and 3150 cm^{-1} on the large profile of the ν_{OH} mode at 3260 cm^{-1}.

Several temperature-programmed desorption (TPD) experiments, adapted to Fourier transform infrared (FTIR) spectroscopy as previously described,[13] were conducted using different β heating rates. For each β heating rate value, we could evaluate the fractional surface coverage from the normalized integrated absorbance of the HC_5N vs T.

Computational Details

To represent the ice surface, two general strategies are available. The molecular cluster method was carried on in our last studies;[14] the ice surface was represented by a *closed* cluster of hydrogen-bonded water molecules, up to 10 units generally. This option enables the use of sophisticated methods and is very

* To whom correspondence should be addressed.

10.1021/jp803524q CCC: $40.75
Published on Web 08/13/2008

TABLE 1: Experimental and Calculated Frequencies of HC_5N[a]

	theory				experiment					
	CCSD(T) anharmonic and harmonic (*italic*)[19]		B3LYP/aug-cc-pVTZ harmonic, scaled[20]		Ar matrix[22]		solid		adsorbed on amorphous ice	
mode	ν (cm^{-1})	intensity (km/mol)	ν (cm^{-1})	intensity (km/mol)	ν (cm^{-1})	relative intensity*	ν (cm^{-1})	relative intensity	ν (cm^{-1})	relative intensity
$\nu_3 + \nu_5$	3334	39.0	3345	n/a	3320.3	15	3227	74	not found	
	3382	n/a								
ν_1	3349	49.0	3321	121	3304.0	60	3209	92	not found	
	3455	*91*								
$2\nu_5$	2262	29.6	2306	n/a	2334.3	12	not found		not found	
	2314	*n/a*								
ν_2	2319	33.6	2256	98	2248.5	45	2251	100	2250	100
	2318	*66*								
ν_3	2198	5.5	2192	2	2186.4	12	2187	18	2187	15
	2225	*3.9*								
n/a							2175	11	2177	14
ν_4	2067	0.08	2061	0	2056.2	1	2049	20	2046	18
	2090	*0.03*								

[a] *Percent intensities (measured with the accuracy of ca. 20%) relative to the strongest band ν_7 (643.6 cm^{-1}).

useful for spectroscopy applications. The less satisfactory aspect is that the solid three-dimensional (3D) boundary conditions cannot be included and also that the very long computation times restrict the system to a very small number of constituents.

Another quantum method can be chosen in the domain of solid-state physics. In this case, the periodic boundary conditions are fully taken into account. The periodic 3D calculations were performed within the framework of the gradient-corrected density functional theory using the *PWscf* computer code from the Quantum-Espresso package.[15] Exchange as well as the correlation functionals are Perdew−Burke−Ernzerhof (PBE). A plane wave basis set used was associated to Vanderbilt ultrasoft pseudopotentials[16] and an energy cutoff of 32 Rydberg (435 eV). The same method was carried out during our study on carbon monoxide adsorption on ice[17] and proved efficient even if the CO−ice interactions are very small. Of course, the plane wave basis set does not generate any problem of BSSE on the binding energy (BE).

The BE of a moiety M (HC_5N, H_2O, etc.) to ice surface is evaluated as

$$\Delta E_{BE} = E(M + H_2O) - E(M) - E(H_2O_{surface}) \qquad (1)$$

This value is also referred in the text as "adsorption energy" or "interaction energy"; the desorption energy in this framework is simply $-\Delta E_{BE}$.

As before, we adopted the ice surface unit cell optimized by the Turin group[18] known as proton ordered "π-ice" model. The supercell is made of a two layer slab containing 32 water molecules.

Results and Discussion

Adsorption and Desorption of HC_5N on Amorphous Ice. The spectrum of solid HC_5N, in the 650−4000 cm^{-1} range, shows four stretching fundamental modes labeled ν_1 to ν_4 (Table 1). These bands observed at 3209, 2251, 2187, and 2049 cm^{-1} have been assigned, respectively, to CH, CN, and two CC stretching modes.[19−23] We observe another band at 3227 cm^{-1} attributed to the combination mode $\nu_3 + \nu_5$ with regard to our previous study.[23] In solid phase, the $2\nu_7$ combination mode expected around 1270 cm^{-1} is not observed, while another intense band located at 2175 cm^{-1} is obtained but not yet assigned.

Amorphous ice displays a weak feature at 3695 cm^{-1}, which is relative to the dangling H mode (d_H).[24] This latter is generally used to follow the adsorption of molecules on ice surfaces. Two other vibrational surface modes exist at 3549 and 3503 cm^{-1} attributed to the d_O and S_4 sites, respectively.[25] The HC_5N adsorption at 10 K on a bare amorphous ice surface induces no change in the d_H position, indicating that no major interaction between d_H and HC_5N exists as with HC_3N.[8]

However, we observe an important modification in the ice spectrum (Figure 1). The position of bulk OH stretching modes at 3230 cm^{-1} is shifted to higher wavenumbers by 10 cm^{-1}. This shift just as in the case of C_4N_2[26] indicates a strong interaction between the HC_5N and the ice film.

During this adsorption, a large band at 3571 cm^{-1} grows. This band is located in the d_O and S_4 sites regions of bare ice. Recent works[25] have shown that CO, CH_4, and rare gas atoms (Ar and Kr) adsorbed on d_O and S_4 sites led to a decrease in the infrared responses of these sites. However, in the case of the C_4N_2 adsorption, an opposite effect was observed. The present results show that HC_5N (just like C_4N_2) interacts mostly with amorphous ice sites other than d_H.

The infrared band shapes and positions of HC_5N modes are almost the same as those observed for the solid HC_5N (Table 1). Contrary to our studies in the argon matrix and those for the bulk HC_5N, we could not detect the ν_1 band of HC_5N deposited on ice, as it was probably masked by the strong OH stretching band of bulk ice.

Figure 2shows selected spectra recorded during the sample warm-up from 10 K to the HC_5N sublimation temperature with a heating rate β of 0.5 K min^{-1}. Starting from 15 K, the band located at 3571 cm^{-1} decreased in intensity, to disappear at 80 K. Above 85 K, the d_H signal began to decrease in intensity and disappeared at 130 K (Figure 2). The latter phenomenon is due to the collapse of amorphous ice pores during their evolution toward crystalline ice. The desorption process of HC_5N can be followed in Figure 3 showing the variations of the ν_2 band intensity. Between 80 and 120 K, the intensity of this band remains unchanged, which is indicative of a stable adsorption state. At 140 K, we observe an abrupt decrease that results from the sublimation of adsorbed HC_5N. It is remarkable that (i) this sublimation occurs at the beginning of the ice crystallization

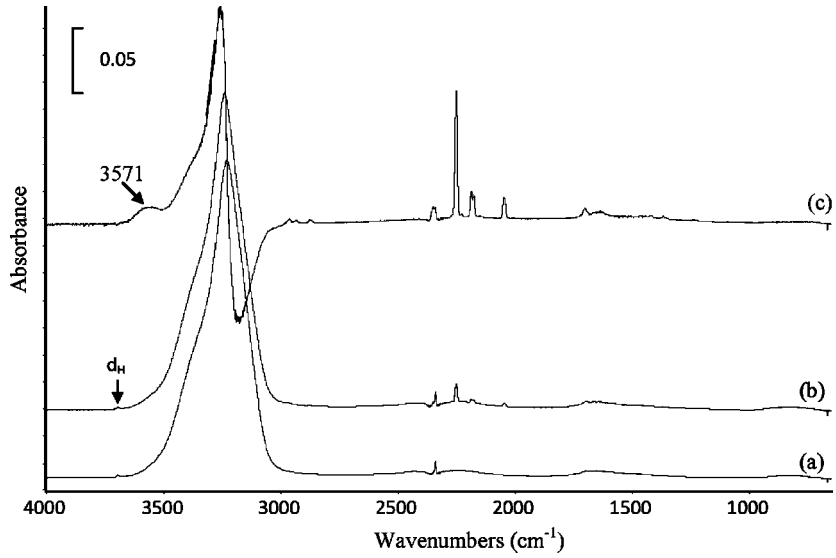

Figure 1. Infrared spectra resulting from a HC_5N exposure on an amorphous ice film maintained at 10 K: (a) Bare amorphous ice, (b) 5 μmol of HC_5N deposited on this ice, (c) substraction spectrum b − a, and spectrum c multiplied by 5.

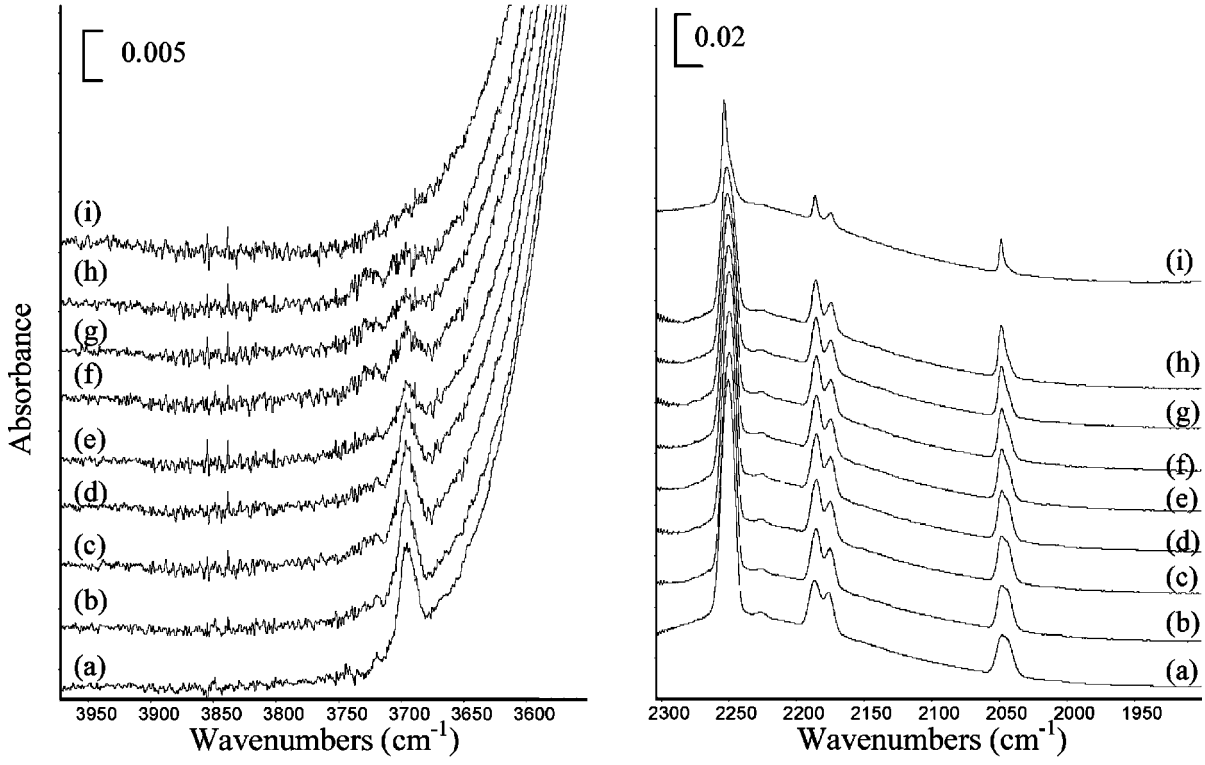

Figure 2. Selected infrared spectra during the TPD (heating rate $\beta = 0.5$ K min^{-1}) of HC_5N from amorphous ice surface in the OH stretching region of ice and in the ν_2, ν_3, and ν_4 mode region of HC_5N: (a) 10, (b) 90, (c) 100, (d) 110, (e) 120, (f) 125, (g) 135, (h) 140, and (i) 155 K.

process near the phase transition temperature and (ii) it occurs at a lower temperature than for bulk HC_5N ($\approx$170 K, Figure 3). Recent studies[8,26] have shown that the sublimation of C_4N_2 adsorbed on ice occurs similarly at approximately 150 K, while that of HC_3N takes place at a lower temperature of 135 K.

Just as for other polyynes, the HC_5N desorption follows a first-order kinetic model. To characterize the interaction energy between HC_5N and amorphous ice surface, we have performed a TPD study. Table 2 lists experimental results obtained using four β heating rate values between 0.3 and 0.9 K min^{-1}. T_p (temperature for which the desorption is maximal) is evaluated for each heating rate. From the linear plot of $\ln \beta/RT_p^2$ vs $1/T_p$ (Figure 4), we have derived the activation energy of desorption, $E_d = 90 \pm 20$ kJ/mol, and the pre-exponential factor $A_d = 10^{13}$ s^{-1}. This E_d value is higher than the one evaluated with TPD for pure solid HC_5N sublimation and different from that of previous reports regarding HC_3N (39 ± 8 kJ/mol)[8] and C_4N_2 (42 ± 5 kJ/mol).[26] At last, the activation desorption energy (90 ± 20 kJ/mol) measured from the HC_5N desorption of the ice surface is consistent with numerous interactions between the ice surface and the HC_5N moiety. Notwithstanding that the two first members of the cyanopolyyne family present some similarity during the complexation observed in cryogenic matrix, the activation desorption energy is very different. Indeed, the HC_5N is the double of HC_3N desorption's energy. This is probably due to the interaction of ice and the Π system, which must be more important in the first case.

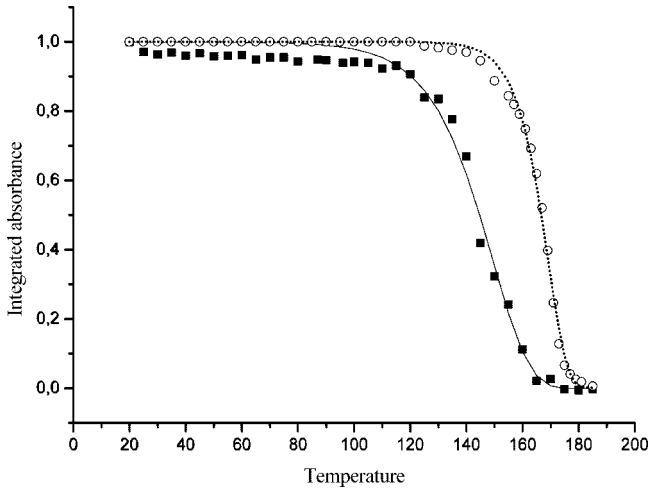

Figure 3. Evolution of integrated normalized absorbance of the ν_2 mode of HC_5N adsorbed on ice surface (square) and for pure HC_5N (ball) with temperature (heating rate $\beta = 0.5$ K min^{-1}).

TABLE 2: Desorption Peak Maximum Temperatures (T_p) for Various Heating Rates (β)

heating rate β (K min^{-1})	T_p (K)
0.3	148.8
0.5	149.4
0.7	150.0
0.9	150.9

When crystalline ice is submitted to a progressive HC_5N exposure, no change in the spectral line shape is observed. The infrared spectrum is similar to that of the HC_5N solid. During the temperature increase, the HC_5N deposited on crystalline ice sublimates around 155 K. No bands are detected in the 3500 cm^{-1} area corresponding to a stable adsorption site.

Quantum Study of HC_5N Adsorption on Water Ice Surface. Our experimental results indicate that HC_5N adsorption does not proceed through on the dangling OH sites of the amorphous ice surface. Theoretical calculations were carried out to model the comportment of HC_5N adsorbed on the amorphous ice surface.

As previously evoked, we adopted the "π-ice" model optimized by the Turin group[18] known as proton ordered. In ref 17 as well as in ref 27, this model of surface proved to be realistic enough to represent accurately the ice−carbon monoxide and acetic acid interaction, although the experiments were performed on amorphous ice surfaces. Nevertheless, these molecules are very small in dimension, and within very short distance, π-ice is a good model of the physical environment. The situation is lightly different with HC_5N, which is more than 7 Å long. Therefore, the optimized structure for adsorption on the bare π-ice surface looks like Figure 5.

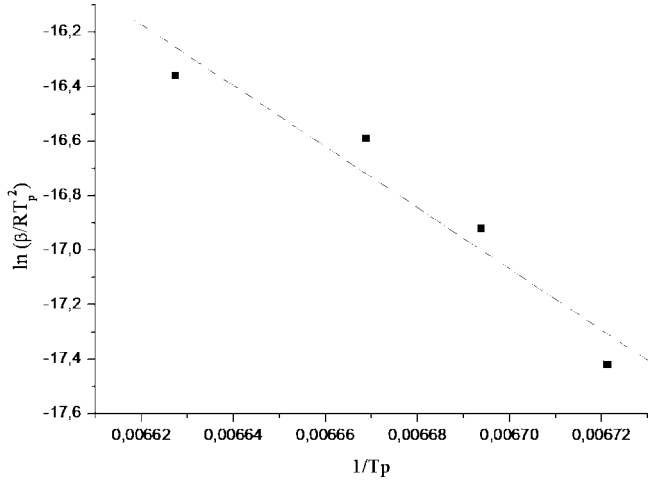

Figure 4. Desorption kinetics of HC_5N from an amorphous ice surface obtained for four TPD experiments. The line is derived from a linear regression analysis of the data points.

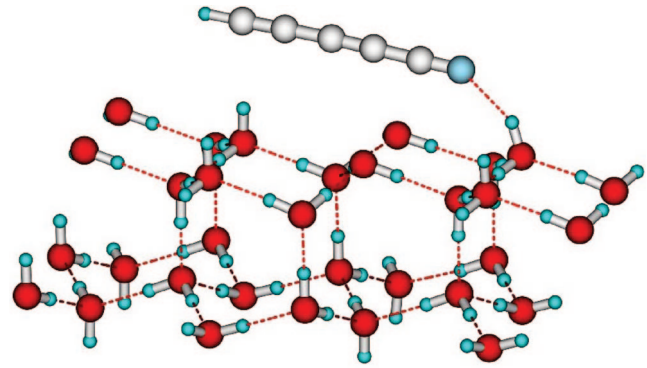

Figure 5. Adsorption of the HC_5N molecule on bare π-ice surface.

The starting structure for geometry optimization featured the HC_5N molecule roughly parallel to the ice surface; the final geometry is displayed in Figure 5. By analogy with the structure of HC_5N:H_2O complexes formed in solid argon,[7] the HC_5N molecule was placed with its terminal hydrogen interacting with a free dangling O of the ice surface, while the terminal nitrogen was in interaction with a free dangling H.

The molecule is bonded to the substrate by only one weak H-bond between the nitrogen atom and the one dangling H. Consequently, the BE is small, −34 kJ/mol, and the interaction with the ice surface is weak on the contrary with our experimental finding.

Because the ice surface is essentially dynamic, water molecules can desorb and readsorb again, thus hydrating the adsorbed HC_5N. Therefore, the idea was to add in sequence extra H_2O on the surface around the molecule. The problem is that the molecule exhibits two hydrophilic zones at its ends, whereas the carbon atoms are less sensitive to water interaction; then, we concentrated our efforts in a model hydration of the N and H atoms. Six water molecules were enough to hydrate N, and ΔE_{BE} dropped down to −70 kJ/mol. Two more waters yield the structure displayed in Figure 6, and the adsorption energy on this perturbed ice surface is now 80 kJ/mol. We can hardly pretend that this structure is really the physical one, but we do pretend that it is a good model for adsorption on a disordered ice surface. The structure of the adsorbed moiety is very slightly affected: The molecule undergoes a curvature and is no more linear, but the bond lengths are not modified. The system stability is ensured by two strong N···H bonds (2.09 and 2.29 Å) and a H···O bond (1.84 Å). Calculating the phonon structure of such a large crystal cell (127 atoms) is hardly possible; therefore, we have tried that on the cluster corresponding to one unit cell. The whole system is calculated using Gaussian 03[28] and the ONIOM model[29] with B3LYP/6-31 g (d,p) for the high-level cluster and AM1 for the low-level cluster.

It is worth-mentioning that the presently described interactions between the HC_5N and the ice surface are very similar to those observed in the argon matrix between HC_5N and water molecules. At last, it is important to note that when HC_5N is adsorbed upright a d_O site, the optimization leads the HC_5N to be parallel to the ice surface.

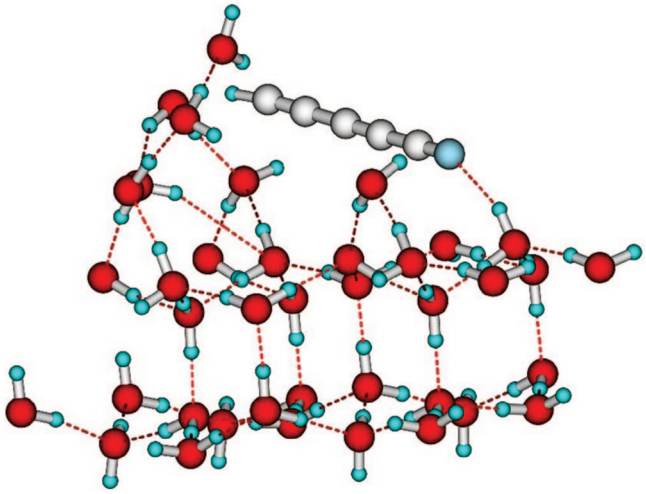

Figure 6. Adsorption and hydration of the HC_5N molecule on π-ice.

TABLE 3: Optimized Structural Parameters for the HC_5N Adsorbed on an Amorphous Ice Surface Obtained by Theoretical Calculations[a]

parameters	free HC_5N	dH sites	HC_5N adsorbed
r N_1C_2	1.17		1.17
r C_2C_3	1.35		1.35
r C_3C_4	1.22		1.23
r C_4C_5	1.34		1.34
r C_5C_6	1.22		1.22
r C_6H_7	1.10		1.11
$\angle N_1C_2C_3$	180.0		177.3
$\angle C_2C_3C_4$	180.0		176.2
$\angle C_3C_4C_5$	180.0		177.5
$\angle C_4C_5C_6$	180.0		178.0
$\angle C_5C_6H_7$	180.0		173.8
rOH		0.97	0.97

[a] Bond lengths are given in Å, and angles are given in degrees.

Table 3 gives the optimized geometrical parameters obtained for HC_5N and for the dangling H sites involved in the hydrogen bonding. These data indicate that the bond lengths of HC_5N adsorbed on water ice are nearly unchanged with respect to the monomer structure. Only the bond angles are modified, deviating from linearity by 2−6°. Consequently, only slight shifts of the infrared absorption bands were detected. It should be recalled that we do not detect any HC_5N bending modes in the present experimental conditions. The molecule undergoes a bending and is no more linear.

Moreover, only the OH bond length of the d_H site in interaction with HC_5N is slightly perturbed by the adsorption (Table 3). This bond is longer than in the bare ice by only 0.001 Å. Considering the clusters that support this calculation, only the d_H previously evoked is considered; in the other site, this mode is assumed to be unaffected.

We can also note that the adsorption of HC_5N on the amorphous water ice leads to dramatic modifications of the ice structure after optimization (Figure 6). This result is consistent with the presently detected infrared absorption frequency shifts for the bulk OH stretching mode. The same phenomenon has already been observed for C_4N_2 adsorbed on the ice surface.[26]

The predicted interaction energy of HC_5N with water ice surface is in the same order of magnitude as the experimental one obtained by the TPD. This lack of accuracy is understandable, given the qualitative character of the applied theoretical model.

Conclusion

According to our measurements of infrared absorption spectra, HC_5N is stable on the ice surface up to the temperature of 150 K, which makes this adsorption interesting for the interstellar medium chemistry. HC_5N is slightly curved on the ice surface and stabilized by a strong hydrogen bond (1.84 Å long) and two strong N···H bonds (2.09 and 2.29 Å). The adsorption of HC_5N on amorphous ice surface induces a strong reorganization of the surface structure. The observation of a new strong band at 3571 cm^{-1} is indicative of a major restructuring of the ice bulk coming from the fact that the amorphous ice is dynamic. This vibrational absorption comes from water molecules, which embed the HC_5N moiety. However, the HC_5N adsorption drives to structural modifications of the ice surface as for C_4N_2. No similar modifications have been reported for the HC_3N adsorption. We can assume that this great ice modification comes from the Π system, which is similar between HC_5N and C_4N_2. In the case of C_4N_2 (like observed for C_3O_2[30]), the absorption induces the growing of a band at 3649 cm^{-1}, which is due to the interaction between the d_H and the nitrogen atoms of C_4N_2. The calculations show that the C_4N_2 or C_3O_2 molecules were flattened on the ice surface, the two terminal atoms interacting with two free OH bonds of the ice surface. No similar interaction has been observed in our experiment.

Acknowledgment. The theoretical part of this work was conducted with the technical means of "Centre régional de Compétence en Modélisation Moléculaire de Marseille". We express our gratitude to Pr. R. Kolos (Institute of Physical Chemistry, Polish Academy of Sciences, Kasprzaka 44, 01-224 Warsaw, Poland) and Dr. Y. Ferro (UMR CNRS 6633, Université de Provence) for the valuable discussions.

References and Notes

(1) Millar, T. J.; Rawlings, J. M. C.; Bennett, A.; Brown, P. D.; Charnley, S. B. *Astron. Astrophys., Suppl. Ser.* **1991**, *87*, 585.

(2) (a) Okabe, H. *J. Chem. Phys.* **1981**, *75*, 2772. (b) Thaddeus, P.; McCarthy, M. C.; Travers, M. J.; Gottlieb, A.; Chen, W. *Faraday Discuss.* **1998**, *109*, 121.

(3) Coustenis, A.; Schmitt, B.; Khanna, R. K.; Trotta, F. *Planet Space Sci.* **1999**, *47*, 1305.

(4) Coustenis, A.; Salama, A.; Lellouch, E.; Encrenaz, Th.; Bjoraker, G. L.; Samuelson, R. E.; de Graauw, Th.; Feuchtgruber, H.; Kessler, M. F. *Astron. Astrophys.* **1998**, *336*, L85.

(5) Avery, L. W.; Broten, N. W.; MacLeod, J. M.; Oka, T.; and Kroto, H. W. *Ap. J. (Lett.)* **1976**, *205*, L173.

(6) Coll, P.; Coscia, D.; Smith, N.; Gazeau, M. C.; Ramírez, S. I.; Cernogora, G.; Israël, G.; Raulin, F. *Planet Sp. Sci.* **1999**, *47*, 1331.

(7) Coupeaud, A.; Piétri, N.; Aycard, J. P.; Couturier-Tamburelli, I. *Phys. Chem. Chem. Phys.* **2007**, *9*, 3985.

(8) Borget, F.; Chiavassa, T.; Allouche, A.; Marinelli, F.; Aycard, J. P. *J. Am. Chem. Soc.* **2001**, *123*, 10668.

(9) Trolez, Y.; Guillemin, J. C. *Angew. Chem. Int.* **2005**, *44*, 7224.

(10) (a) Givan, A.; Loewenshuss, A.; Nielsen, C. *J. Phys. Chem. B* **1997**, *101*, 8696. (b) Givan, A.; Loewenshuss, A.; Nielsen, C. *J. Chem. Phys. Lett.* **1997**, *275*, 98.

(11) Rowland, D.; Devlin, J. P. *J. Chem. Phys.* **1991**, *94*, 812.

(12) Graham, J. D.; Roberts, J. T. *Geophys. Res. Lett.* **1995**, *22*, 251.

(13) Couturier-Tamburelli, I.; Chiavassa, T.; Pourcin, J. *J. Phys. Chem. B* **1999**, *103*, 3677.

(14) (a) Allouche, A. *J. Phys. Chem. A* **1999**, *103*, 9150. (b) Ferro, Y.; Allouche, A. *J. Chem. Phys.* **2003**, *118*, 10461. (c) Ferro, Y.; Allouche, A.; Kempter, V. *J. Chem. Phys.* **2004**, *120*, 8683.

(15) Scandolo, S.; Giannozzi, P.; Cavazzoni, C.; de Gironcoli, S.; Pasquarello, A.; Baroni, S. *Z. Kristallogr.* **2005**, *220*, 574; Quantum Espresso website http://www.quantum-espresso.org.

(16) Laasonen, K.; Pasquarello, A.; Lee, C.; Car, R.; Vanderbilt, D. *Phys. Rev. B* **1993**, *47*, 10142.

(17) Manca, C.; Martin, C.; Allouche, A.; Roubin, P. *J. Phys. Chem. B* **2001**, *105*, 12861.

(18) (a) Pisani, C.; Casassa, S.; Ugliengo, P. *Chem. Phys. Lett.* **1996**, *253*, 201. (b) Casassa, S.; Ugliengo, P.; Pisani, C. *J. Chem. Phys.* **1997**, *106*, 8030.

(19) Botschwina, P.; Oswald, M. *Spectrochim. Acta* **1997**, *A53*, 1097.

(20) Gronowski, M.; Kołos, R. *Chem. Phys. Lett.* **2006**, *428*, 245.

(21) Benilan, Y.; Ferraday, T.; Fray, N.; Jolly, A.; Raulin, F.; Guillemin, J. C. *Bull. Am. Astron. Soc.* **2005**, *37*, 717.

(22) Coupeaud, A.; Kołos, R.; Couturier-Tamburelli, I.; Aycard, J. P.; Piétri, N. *J. Phys. Chem. A* **2006**, *110*, 2371.

(23) Coupeaud, A.; Turowski, M.; Gronowski, M.; Piétri, N.; Couturier-Tamburelli, I.; Kołos, R.; Aycard, J. P. *J. Chem. Phys.* **2007**, *126*, 164301.

(24) Mayer, E.; Pletzer, R. *Nature* **1986**, *319*, 298.

(25) (a) Manca, C.; Martin, C.; Roubin, P. *Chem. Phys.* **2004**, *300*, 53. (b) Manca, C. Thesis of Université de Provence, 2002. (c) Manca, C.; Martin, C.; Allouche, A.; Roubin, P. *J. Phys. Chem. B* **2001**, *105*, 12861.

(26) (a) Guennoun, Z. Thesis of Université de Provence, 2004. (b) Guennoun, Z.; Couturier-Tamburelli, I.; Piétri, N.; Aycard, J. P. *J. Phys. Chem. B* **2005**, *109*, 3437.

(27) Allouche, A.; Bahr, S. *J. Phys. Chem. B* **2006**, *110*, 8640.

(28) Frisch, M. J.; Trucks, G. W.; Schlegel, H. B.; Scuseria, G. E.; Robb, M. A.; Cheeseman, J. R.; Montgomery, J. A., Jr.; Vreven, T.; Kudin, K. N.; Burant, J. C.; Millam, J. M.; Iyengar, S. S.; Tomasi, J.; Barone, V.; Mennucci, B.; Cossi, M.; Scalmani, G.; Rega, N.; Petersson, G. A.; Nakatsuji, H.; Hada, M.; Ehara, M.; Toyota, K.; Fukuda, R.; Hasegawa, J.; Ishida, M.; Nakajima, T.; Honda, Y.; Kitao, O.; Nakai, H.; Klene, M.; Li, X.; Knox, J. E.; Hratchian, H. P.; Cross, J. B.; Bakken, V.; Adamo, C.; Jaramillo, J.; Gomperts, R.; Stratmann, R. E.; Yazyev, O.; Austin, A. J.; Cammi, R.; Pomelli, C.; Ochterski, J. W.; Ayala, P. Y.; Morokuma, K.; Voth, G. A.; Salvador, P.; Dannenberg, J. J.; Zakrzewski, V. G.; Dapprich, S.; Daniels, A. D.; Strain, M. C.; Farkas, O.; Malick, D. K.; Rabuck, A. D.; Raghavachari, K.; Foresman, J. B.; Ortiz, J. V.; Cui, Q.; Baboul, A. G.; Clifford, S.; Cioslowski, J.; Stefanov, B. B.; Liu, G.; Liashenko, A.; Piskorz, P.; Komaromi, I.; Martin, R. L.; Fox, D. J.; Keith, T.; Al-Laham, M. A.; Peng, C. Y.; Nanayakkara, A.; Challacombe, M.; Gill, P. M. W.; Johnson, B.; Chen, W.; Wong, M. W.; Gonzalez, C.; Pople, J. A. Gaussian 03, revision B.04; Gaussian, Inc.: Wallingford, CT, 2004.

(29) Dapprich, S.; Komaromi, I.; Byun, K. S.; Morokuma, K.; Frisch, M. J. *J. Mol. Struct. Theochem.* **1999**, *461*, 1.

(30) Allouche, A.; Couturier-Tamburelli, I.; Chiavassa, T. *J. Phys. Chem. B* **2000**, *104*, 1497.

JP803524Q